International Journal of Science and Research (IJSR)
ISSN (Online): 2319-7064
Index Copernicus Value (2016): 79.57 | Impact Factor (2015): 6.391

Effect of Relative Density on Liquefaction Potential of Sandy Soil from Small Laboratory Machine Foundation Model

Mohammed Y. Fattah[1], Nahla M. Salim[2], Rusul J. Haleel[3]

[1]Professor, Building and Construction Engineering Department, University of Technology, Baghdad, Iraq

[2]Assistant Professor, Building and Construction Engineering Department, University of Technology, Baghdad, Iraq

[3]Graduate student, Building and Construction Engineering Department, University of Technology, Baghdad, Iraq

Abstract: ***Liquefaction is a phenomenon that occurs during earthquakes, and leads to ground failure. Water-saturated, well sorted, fine grain sands and silts behave as viscous fluid as a result of liquefaction. This behavior of fluids is very different than solids behavior. This paper presents and discusses the results of 54 experimental model tests, all of them were performed on saturated sand under vertical dynamic traffic load using different relative densities (medium and dense), different shapes of footing (square and circular), and different embedment depths (at surface and at depth B) where B is the width of footing. It was concluded that by increasing the relative density of sand, the surface settlement decreases; when sand's relative density increases from 60% to 80%, the reduction of the surface settlement for surface footing condition was about 26 to 72 % at (0.5 ton, 0.5 Hz – 2 ton, 1 Hz), and 27 – 74 % at (0.5 ton, 0.5 Hz – 2 ton, 1 Hz) reduction for embedded footing condition models. Also the embedment of footing in dense sand reduces the settlement more than medium sand, because the dense soil is the stiffest. The amplitude of displacement (Az) decreased at both depths B and 2B, when soil relative density increased, the percentage of reduction in (Az) was about (4-93) % at depth B, and about (37-77) % at depths 2B, when soil relative density increased from (60%) to (80%). Also the displacement amplitude (Az) of the surface square footing is less than that of circular footing at both depths B and 2B.***

Keywords: Liquefaction; machine foundation; sand; relative density; frequency

1. Introduction

Soils are periodically subjected to dynamic loads in many circumstances, such as earthquakes, storm waves for offshore structures, wind forces in high buildings, pile construction, traffic loads and machine vibrations.

Liquefaction is a term used repeatedly to characterize a special type of failure of saturated soils (silt and sand) when they are subjected to static or cyclic loading. The interaction of soil and pore fluid under loading may lead to the buildup of pore pressure, which results in soil softening and loss of shear strength. In extreme case, the soil loses all the shearing resistance and fails like a viscous liquid, a process known as 'liquefaction' (Taiebat et al., 2007).

Sladen et al., (1985) defined liquefaction as "a phenomenon wherein a mass of a soil loses a large percentage of its shearing resistance, when subjected to monotonic, cyclic or shock loading, and flows in a manner like a liquid until the shear stresses acting on the mass are as low as the reduced shearing resistance".

Casagrande (1936) was the first one who studied the importance of liquefaction of sands induced by static loading, while liquefaction of sands induced by seismic loading had a great deal of attention at 1964 when two major earthquakes shook Anchorage, Alaska, and Niigata, Japan, resulting in substantial damage and loss. The Alaska earthquake, a shock with a magnitude, M, of 9.2 on the Richter scale, has damaged more than 200 bridges and has caused huge landslides. During the 7.5-magnitude earthquake of June 16, 1964, in Niigata, Japan, the extensive liquefaction of sand deposits caused major damage to buildings, bridges, highways and utilities. It was estimated that more than 60,000 buildings and houses were destroyed (GDP-9, 2007).

Sand is said to be liquefied and has no shear strength when drainage is impossible, and the pore water pressure (u) rises with constant total stress (σ_v) up to $\sigma_v = u$, after that the effective stress σ'_v will be equal to zero. The contact force between soil particles become very small or zero due to high pore water pressure, and in an excessive case, the excess pore water pressure can rise to a value that can break the particle-to-particle contact. In such cases, the soil will exhibit very little or no shear resistance, and behave more like a viscous liquid. If it is expressed in Mohr Columb's soil shear strength formulation, it is given as (Das and Ramana, 2011):

$$\tau = c' + \sigma'_v \tan \phi' \quad \text{..... (1)}$$

$$\sigma'_v = \sigma_v - u \quad \text{..... (2)}$$

where: τ : soil shear strength,
c': undrained soil cohesion,
σ_v: total vertical stress,
σ'_v: effective vertical stress,
u: pore water pressure, and
ϕ' : effective angle of internal friction.

In general, liquefaction requires three conditions: (*i*) loose to medium dense cohesionless (sandy) soils, (*ii*) relatively shallow ground water table to ensure full saturation, and (*iii*) strong enough ground motion or cyclic loading (Omarov, 2010).

Fattah et al. (2014) studied predicting liquefaction potential and pore water pressure under the dynamic loading on fully

saturated sandy soil using the finite element method by QUAKE/W computer program. As a case study, machine foundations on fully saturated sandy soil in different cases of soil densification (loose, medium and dense sand) are analyzed. Harmonic loading was used in a parametric study to investigate the effect of several parameters including: the amplitude frequency of the dynamic load. Emphasis was made on zones at which liquefaction takes place, the pore water pressure and vertical displacements develop during liquefaction. The results showed that liquefaction and deformation develop fast with the increase of loading amplitude and frequency. Liquefaction zones increase with the increase of load frequency and amplitude.

The aims of this paper are obtaining the relation between liquefaction potential and soil properties (relative density), in addition to foundation depth and shape and studying the effects of dynamic load parameters (load frequency, amplitude), sand density, embedment depth and footing shape on liquefaction potential.

Testing Program

The number of model tests is 54, which are arranged in two groups, were performed in sand prepared at two relative densities which are (60% and 80%) conformable to medium and dense sand densities, respectively. all model tests were carried outunder dynamic load on saturated sand.

The first group of medium sand consists of 36 models, while the second group of dense sand consists of 18 models, the model tests can be summed up as follows:

a) Thirty six models were tested on saturated medium sand under three load amplitudes conformable to(0.5, 1, 2) ton and three frequencies (0.5, 1, 2) Hz, the sand models were tested with square or circular foundation placed on the surface or embedded at depth B (where B is the width of the footing) for each load amplitude and frequency.
b) Eighteen models were tested on saturated dense sand under three load amplitudes (0.5, 1, 2) ton and three frequencies (0.5, 1, 2) Hz, the sand models were tested with square foundation placed on the surface or embedded at depth B for each load amplitude and frequency.

Soil proprieties

Soil used in this study was sand and obtained from Karbala city west of Baghdad in Iraq. The properties of thesand with two different densities; medium and dense were obtained from standard tests. The physical properties of the used soil are summarized in Table 1. The soil is classified as poorly graded sand with symbol (SP) according to the Unified Soil Classification System (USCS).

Table 1: Physical properties of the used soil

Physical properties		Value	Specification
Specific gravity (Gs)		2.66	ASTM D 854
D_{10} (mm)		0.23	ASTM D 422 and ASTM D 2487
D_{30} (mm)		0.42	
D_{60} (mm)		1.15	
Coefficient of uniformity (Cu)		5	
Coefficient of curvature (Cc)		0.66	
Soil classification		SP	
Maximum void ratio		0.66	-------
Minimum void ratio		0.4	-------
Maximum dry unit weight (γdry)max (kN/m^3)		19	ASTM D 4253
Minimum dry unit weight (γdry)min (kN/m^3)		16	ASTM D 4254
Angle of internal friction at (R.D = 60%)	Dry	41º	ASTM D 3080
	saturation	35.6º	
Angle of internal friction at (R.D = 80%)	Dry	43.5º	
	saturation	37.4 º	

2. Setup Design of Dynamic Load Machine

To study the liquefaction potential in saturated sand, it is essential to emulate the conditions of test as near as possible to field conditions. In order toobtain this aim, a particular testing device. The device has the ability of applying dynamic loads with different load amplitudes and different frequencies, Figure 1 shows the view of the testing advice.

The device, which was manufactured by Abd Al kareem (2013) and modified by Aswad (2016), contains the following parts:

1) Loading steel frame.
2) Axial loading system
3) Model footing,
4) Data acquisition system.
5) Shaft encoder.
6) Steel container.

Figure 1: The loading device

1) Steel loading frame

A steel frame was designed and builtfor supporting and ensuring the verticality of the hydraulic jack which is used for applying the central concentrated load, as shown in Figure 1. The frame consists of 4 columns and 4 beams. All members were made of steel with wall thickness of 4 mm a square cross sectional area of (100×100) mm. The dimensions of the load frame are (1700 × 700 ×1700) mm as a (length× width× height).

To strengthen and support the steel frame, two steel beams were added, as shown in Figure 2 part No. 4.

To hold the system of hydraulic jack and the Encoder which is the device that measure the settlement, a steel plate with dimensions of (700×500) mm and thickness of 20 mm was welded in the center of the frame, as shown in Figure 3. In addition four base plates of dimensions (200 ×200 ×20)mm were used to fix the steel frame with the floor base. All base plates were fixed to the floor by using four bolts with diameter equal to16 mm.

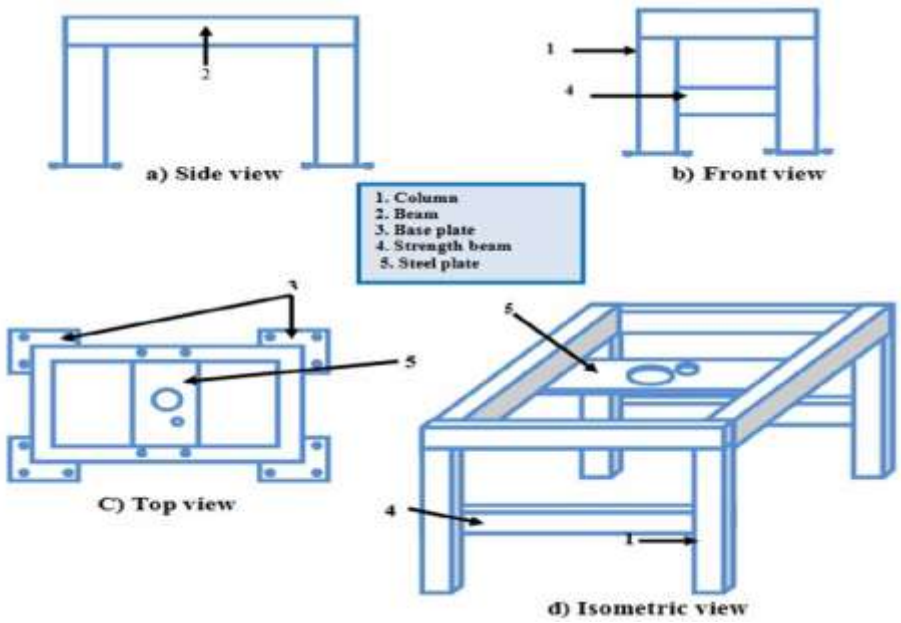

Figure 2: Loading steel frame (after Abed Al-Kareem, 2013).

Figure 3: Steel plate to support the hydraulic jack

2) Axial loading system

It contains of two parts:

1) Hydraulic jack system: this system contains of a hydraulic steel tank with a gage up to 70 liters. The tank contains of two holes; the upper hole is used for filling the oil while the lower one is used for discharge. In addition the tank contains of a hydraulic pump giving a discharge of about 12 liter/min with a maximum pressure of 150 bars.
2) Hydraulic control system: This system is answerable for applying the dynamic loading by using a valve, and the movement of the piston, as shown in Figure 4. A logic control (PLC) is used to control the movement of the hydraulic cylinder jack(up and down), this movement can be controlled by select the hearts through data acquisition.

3) Model footing

To simulate a machine foundation, a square footing made of steel of dimensions (100 ×100) mm and thickness of 20 mm was used, in addition a circular footing of 100 mm diameter was also used.

4) Data acquisition

To measure and sense the displacement that occurring during the tests; data acquisition system is used, which enable the operator to gain a massive readings in a very short time, furthermore, it is used for choosing particular frequency in the test. The data acquisition system is used to analyze the data digitally by Programmable Logic Controller (PLC) which is a digital computer used for electro-mechanical automation processes. PLC device includes LCD touch-screen panel which is used for viewing the input and output data by simplified ladder logic. This LCD is accompanied by three- push buttons to guide the tester for commands related to the test, and enable the tester to use a simple windows for programming the input requirement and saving the results into the computer for calculation.

5) Shaft encoder

The shaft encoder can be defined as an electro-mechanical apparatus which transforms the angular positions (motion) of the shaft to an analog (digital) code. The output of incremental encoder supplies information about the motion of the shaft that is typically further processed elsewhere into information such as speed, displacement, revolution per minute, and position.

6) Steel Container

The experimental tests were performed in a cubic tank made of steel of dimensions (800 x 800 x 800) mm, and thickness of 6 mm.

The strength of the cubic tank has been ensured by adding three steel sections(U-sections) soldered around the tank's sides. In addition the tank has a slick back and front faces. The tank was compatible with loading steel frame which was connected to automatically operate hydraulic jack. A cork with 30 mm thick was used to cover the inside faces of the tank, this cork is used as an absorbing layer and damper to reduce the transmitted waves of the applied dynamic load to the box walls during the test, in addition a rubber with 2.5 mm thickness used to save the cork during preparation of the test. Figure 5 shows the used container.

Figure 4: The hydraulic control system

Figure 5: Steel container

The amplitude of vertical displacement of the points below the foundation at depths (B) which is the width of footing and (2B) are measured. The vibration meter is manufactured locally to measure high displacements in three directions (x, y, and z).

During the tests, two vibration meters are used to measure the amplitude of displacement. The vibration meters are shown in Figure 6.

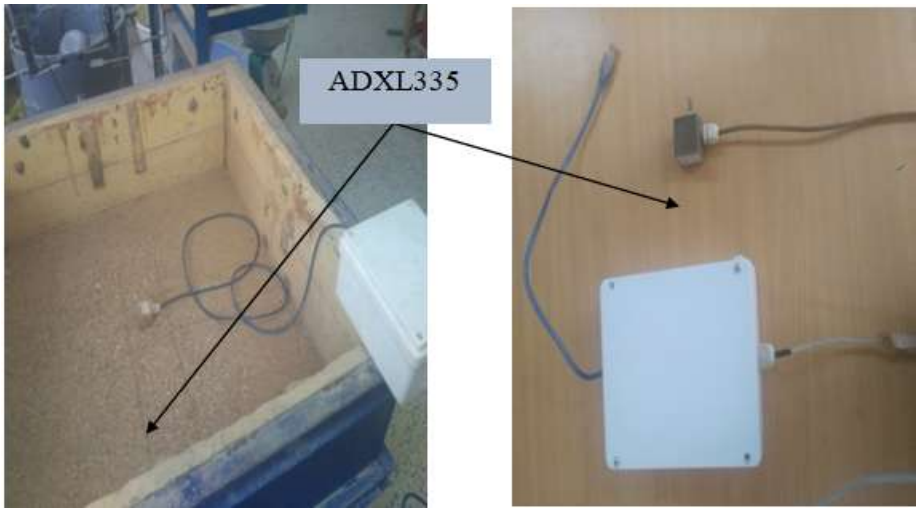

Figure 6: Vibration meter.

Sand Deposit Preparation

A steel tamping hummer was fabricated for preparation sand deposit. According to the used relative densities which are (60% for medium sand and 80% for dense sand), the weight of each layer is predetermined since the unit weight of soil and the volume of the container layers are known also (the container height was divided into 6 equal layers of 100 mm thickness for each layer).

The soil was compacted to a predetermined volume for each layer. After that, the vibration meter probe was installed above a plate (60 * 60) mm at depth (B) and (2B) from the foundation which are equal to 100 mm and 200 mm, then the final layer of soil was completed.

After that, a sharp edge ruler was used to level the top surface of soil to gain as close as possible a flat surface. The footing was then putted in contact with the top surface of the soil model. Finally; the process of saturation of the soil was performed by flowing the water upward(from the bottom of the model to the top surface of soil)at a constant head to prevent the piping potential.

Saturation was carried out by submerging the soil layers for about1 hour. Surplus water at the surface was extracted by using a sponge and water level in the tank was kept in flush with top surface of sand, Figure 7 presents the steps of the sand deposit preparation.

Figure 7: Preparation stages of the test model

3. Presentation and Discussion of Laboratory Test Results

Effect of relative density on the surface settlement

The measured settlement represents the final reduction in the thickness of the soil under the footing. Three different load amplitude were selected, which are (0.5, 1, 2) ton and three different frequencies were used, which are (0.5, 1, 2) Hz. For comparison, each saturated model test was tested with surface footing and embedded footing under the same other situations (relative density, shape of footing, etc.).

Figures 8 to 13 show the relation between the surface settlement and time for square and circle footing models in medium and dense saturated sand. It can be clearly seen that the curves follow the same trend, and the surface settlement raises with raise in load amplitude, in addition, the rate of settlement rising in medium sand is greater than that of the

dense sand. However, this rising is a result to increase in particle stresses.

From figures and Table 2 which presents the surface settlement of saturated sand at different frequencies, load amplitudes, and time, it can be clearly seen that the time to reach a settlement of about 300 mm (the capacity of hydraulic jack of dynamic load set up which is used in tests is 300 mm) decreases as the load amplitude and frequency increase. As shown in figures, the time of tests is varying between (17.22-180) seconds and because of this difference in time among the tests.

Figures 8 to 13 illustrate the influence of sand's relative density on the surface settlement under various load amplitudes and frequencies.

Generally, by increasing sand's relative density, the surface settlement decreases, when the relative density of the soil increases from 60% to 80%, the reduction of the surface settlement for surface footing condition was about 26 to 72 % at (0.5 ton, 0.5 Hz – 2 ton, 1 Hz), and 27 – 74 % at (0.5 ton, 0.5 Hz – 2 ton, 1 Hz) reduction for embedded footing condition models.

Also it is observed that, the embedment of footing in dense sand reduces the settlement more than medium sand, because the dense soil is the stiffest.

In addition to the above-mentioned remarks, it can be noticed that an accumulation of settlement with time was recorded, also it was found that the settlement of the all tests increased rapidly to reach, at time 17.22 seconds, about (33 – 299) % of the width or diameter of footing used; therefore, the failure has been occurring because of occurrence of final liquefaction in the saturated sand beneath the square and circular footing.

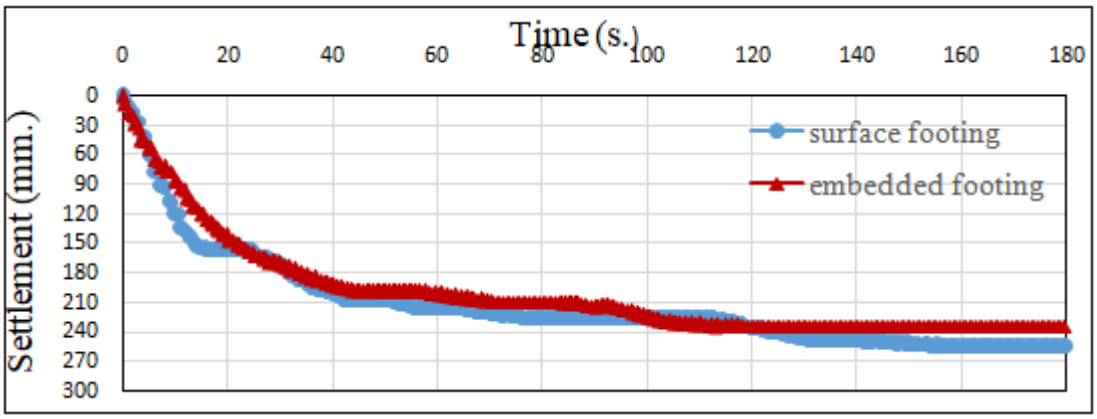

Figure 8: Surface settlement versus time of a square surface and embedded footing, under a =0.5 ton, ω = 0.5 Hz and RD. = 60%.

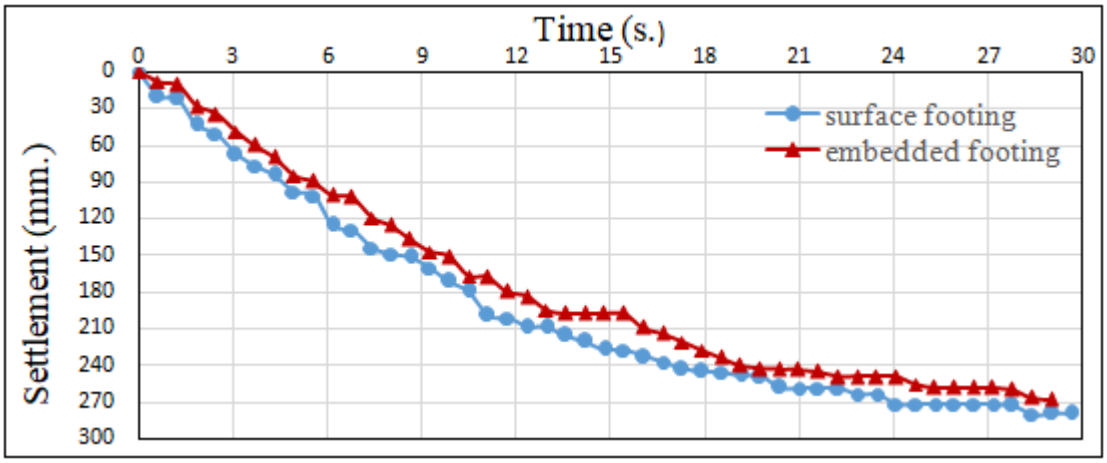

Figure 9: Surface settlement versus time of a square surface or embedded footing, under a = 1 ton, f = 1 Hz and R.D. = 60%.

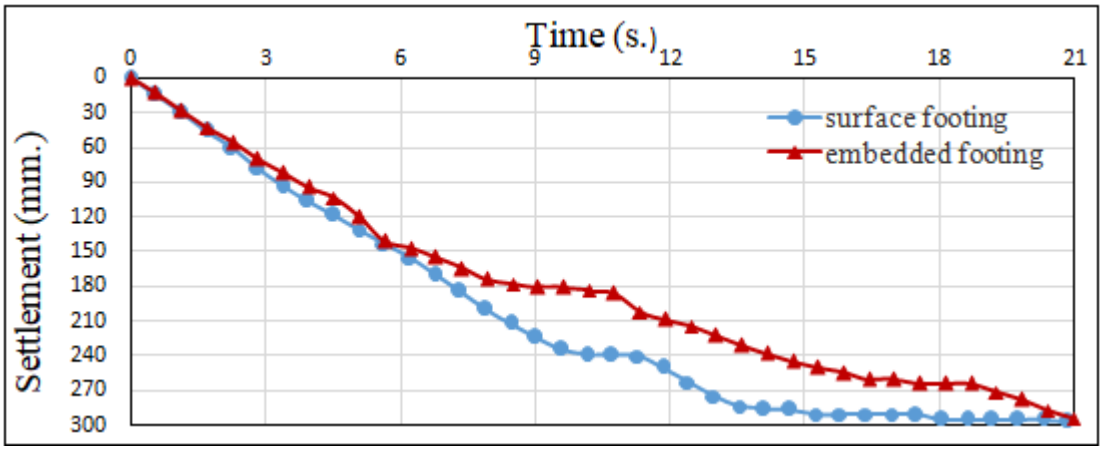

Figure 10: Surface settlement versus time of a square surface or embedded footing, under a = 2 ton, f = 2 Hz and R.D. = 60%.

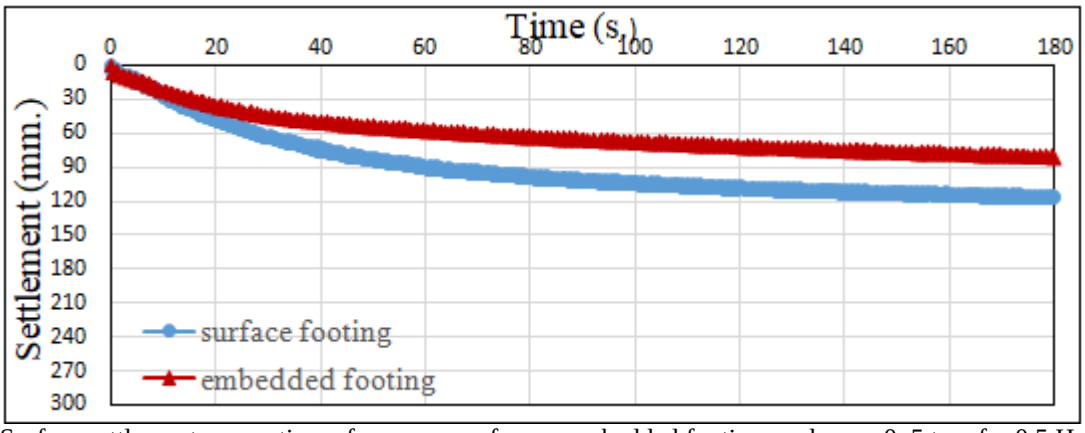

Figure 11: Surface settlement versus time of a square surface or embedded footing, under a = 0. 5 ton, f = 0.5 Hz and R.D. = 80%.

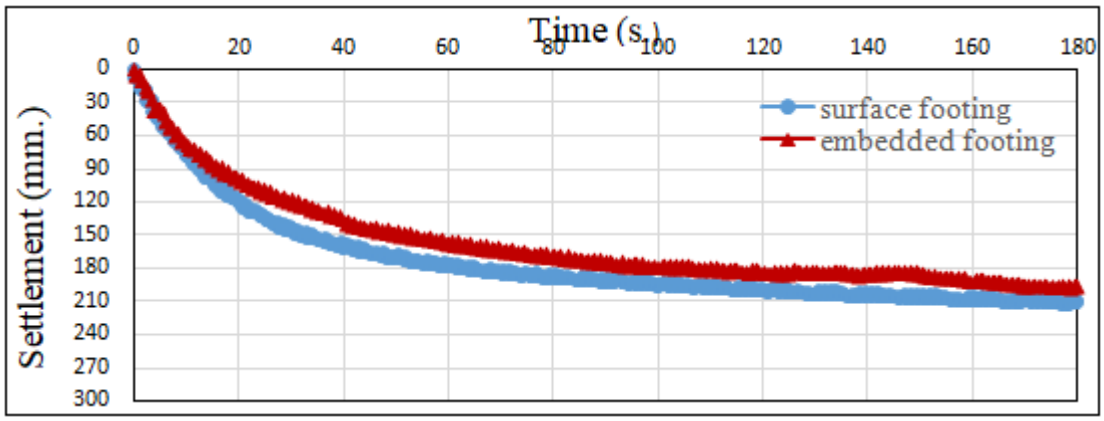

Figure 12: Surface settlement versus time of a square surface or embedded footing, under a = 1 ton, f = 1 Hz and R.D. = 80%.

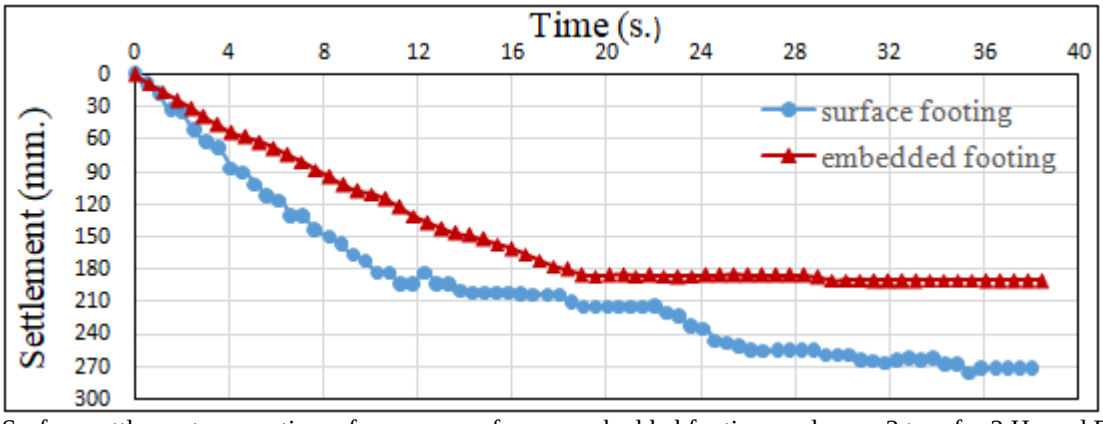

Figure 13: Surface settlement versus time of a square surface or embedded footing, under a = 2 ton, f = 2 Hz and R.D. = 80%.

Table 2: Maximum surface settlement of a footing on saturated sand at different load amplitudes, frequencies, and times

State of soil	Load amplitude (ton)	Surface settlement at different frequencies and times (mm)					
		0.5 Hz	Time (sec)	1 Hz	Time (sec)	2 Hz	Time (sec)
Settlement of surface square footing							
Medium	0.5	254.54	180	260.63	180	299.769	72.18
Dense		117.84	180	178.16	180	201.95	180
Medium	1	279.22	31.67	279.2	29.64	284.27	28.41
Dense		196.95	180	211.42	180	253.33	180
Medium	2	295.07	23.40	292	22.68	296.56	20.87
Dense		200.43	74	295.55	47.86	271.6	38
Settlement of embedded square footing							
Medium	0.5	233.10	180	255.17	180	253.03	72.18
Dense		81.83	180	117.02	180	135	180
Medium	1	242.77	31.67	268.38	29.64	269	28.41
Dense		164.98	180	197.32	180	216.94	180
Medium	2	250.27	23.40	290.09	22.68	293.65	20.87
Dense		168.01	74	176.66	47.86	189.974	38
Settlement of surface circular footing							
Medium	0.5	275.24	67	296.35	40.53	297.8	31.03
Medium	1	277.95	25.24	285.62	24	289	21.15
Medium	2	291.78	20.68	298.45	17.4	299.85	17.22
Settlement of embedded circular footing							
Medium	0.5	188.37	67	218.62	40.53	231.17	31.03
Medium	1	148.54	25.24	243.89	24	258.23	21.15
Medium	2	239.65	20.68	241.86	17.4	268.74	17.22

Effect of sand relative density on displacement at depths B and 2B below the footing

Figures 14 and 15, and Table 3 show the variation of displacement amplitude (A_z) of saturated sand with time at various load amplitudes and relative densities.

It can be clearly seen that, by increasing sand's relative density, the amplitude of displacement (A_z) decreased at both depths (B and 2B). The percent of reduction in (A_z) when the soil relative density increased from (60%) to (80%) was about (4-93) % at depth B, and about (37-77) % at depth 2B for surface footing. This behavior is due to the increase in the stiffness and the modulus of elasticity of dense sandy soil that makes the soil stiffer and resist vibrations.

An exception of the mentioned conclusions is noticed when the load amplitude is 1 ton, frequency 0.5 Hz at depth B with embedded square footing, and when the load amplitude is 1 ton, frequency 0.5 Hz with surface square footing, and load amplitude 0.5 ton, frequency 2 Hz with embedded square footing at depth 2B.

These results are compatible with those found by Fattah et al. (2016) who concluded that the maximum displacement amplitude of footing is reduced to half when the size of footing is doubled for dry and saturated sand. The final settlement of the foundation increases with increasing the amplitude of dynamic force, operating frequency and degree of saturation. Meanwhile, it is reduced with increasing the relative density of sand, modulus of elasticity, and embedding inside soils. The excess pore water pressure increases with increasing the relative density of the sand, the amplitude of dynamic loading and the operating frequency. In contrast, the rate of dissipation of the excess pore water pressure during dynamic loading is more in the case of loose sand.

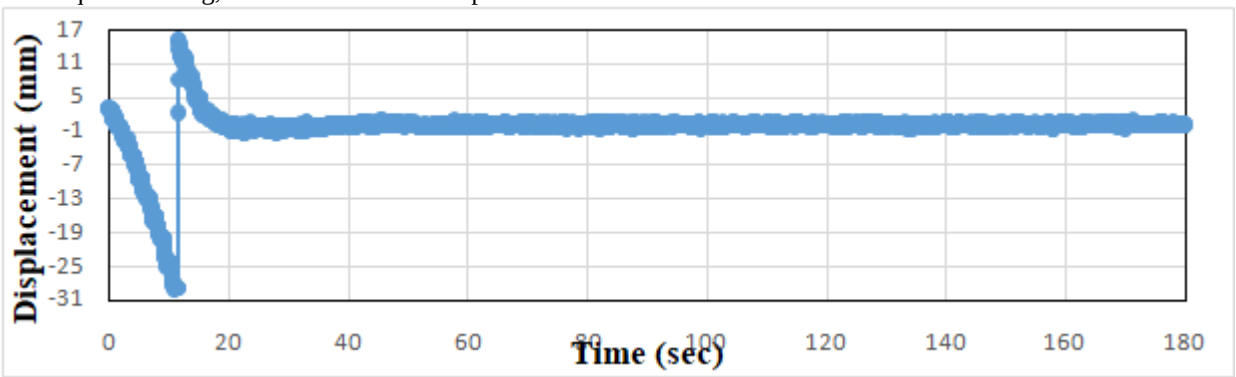

(a): displacement of surface footing at depth B

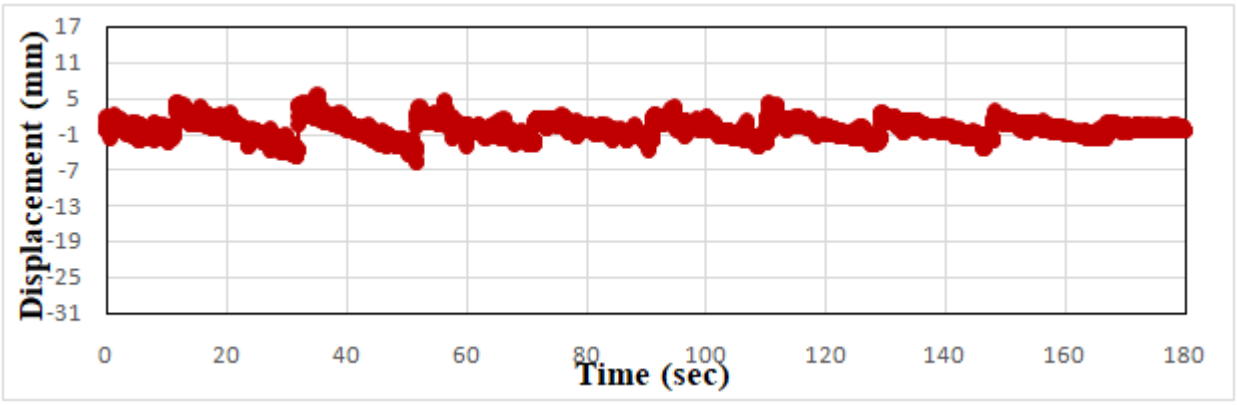

(b): displacement of surface footing at depth 2B

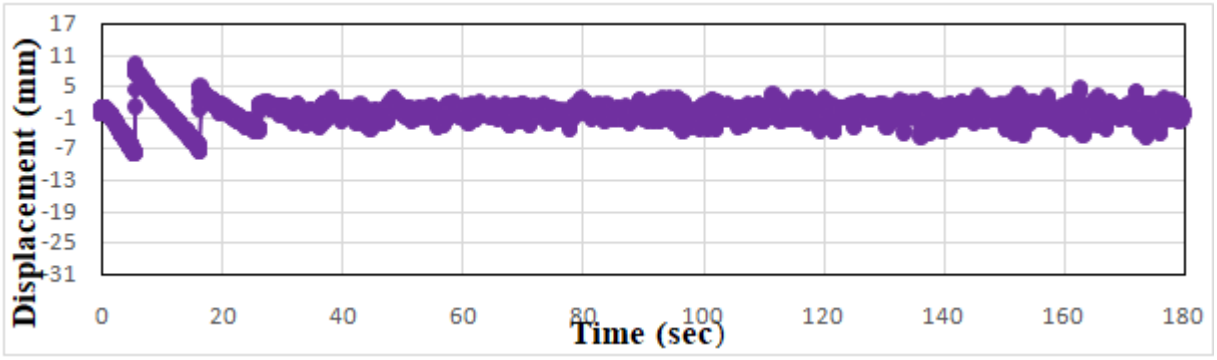

(c): displacement of embedded footing at depth B

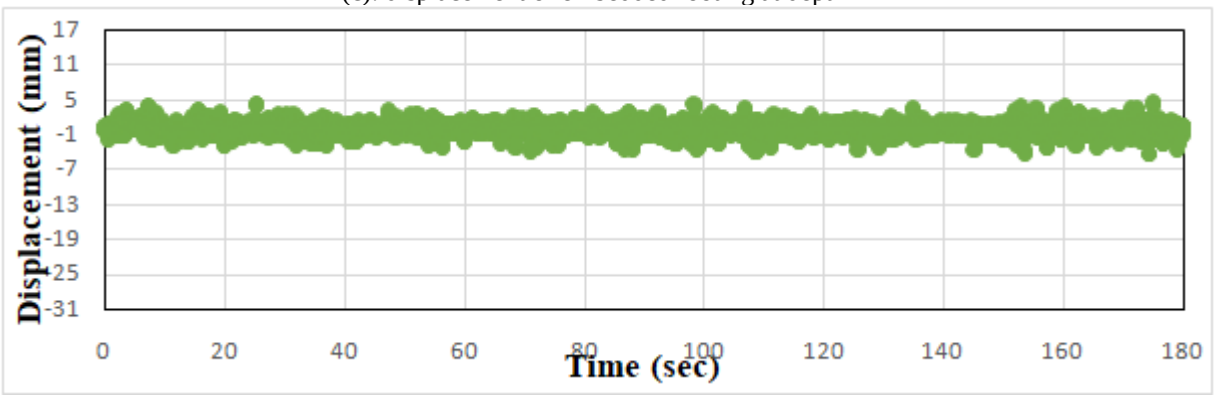

(d): displacement of embedded footing at depth 2B

Figure 8: Variation of the displacement at depths B and 2B with time under a = 0.5 ton, f = 0.5 Hz and R.D. = 60%, under a square surface and embedded footing.

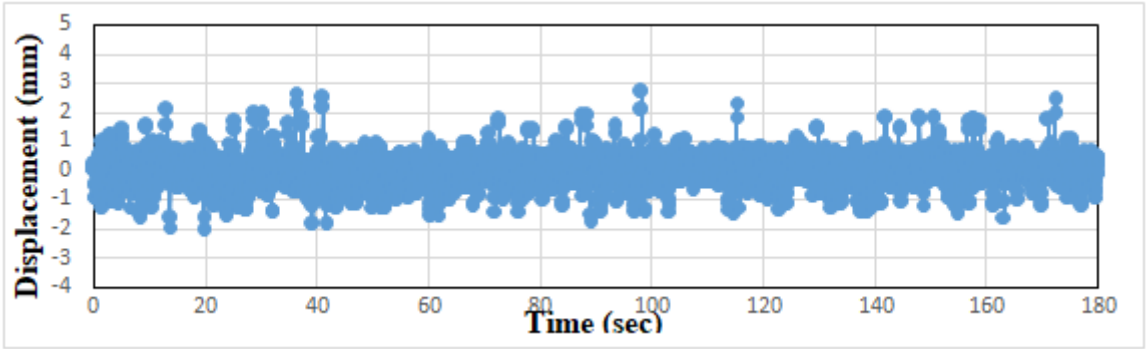

(a): displacement of surface footing at depth B

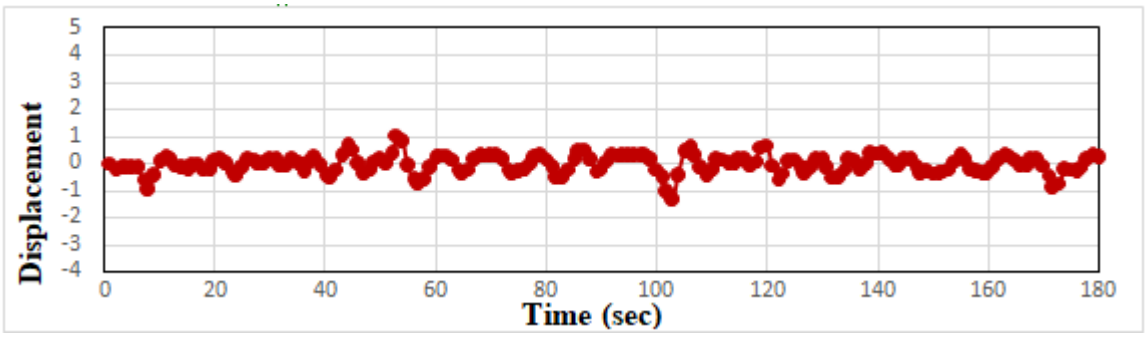

(b): displacement of surface footing at depth 2B

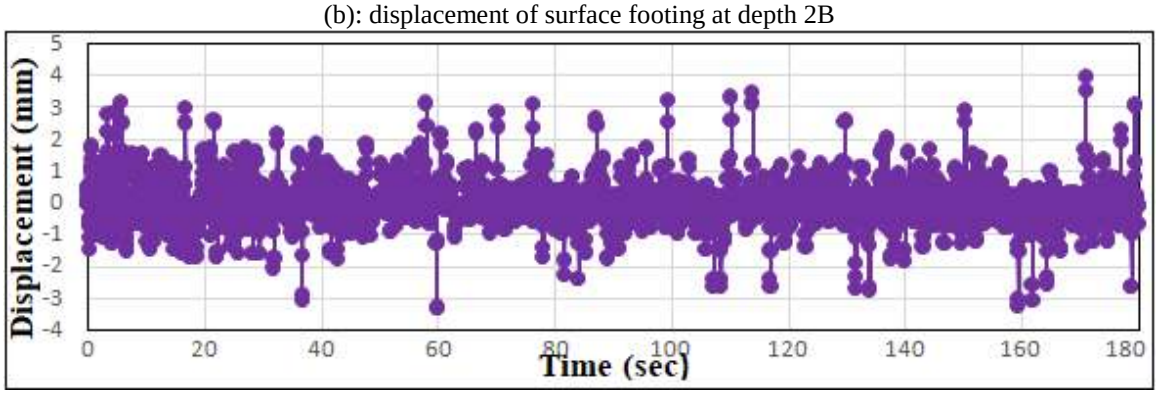

(c): displacement of embedded footing at depth B

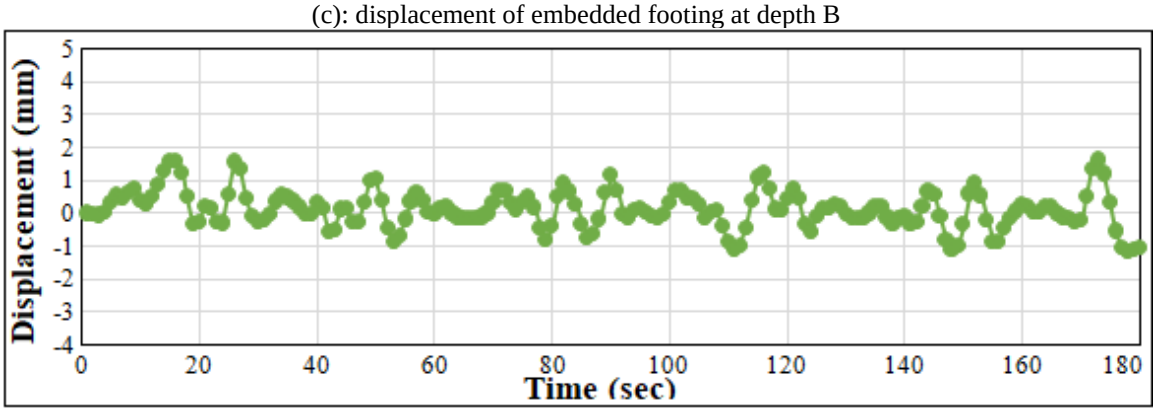

(d): displacement of embedded footing at depth 2B

Figure 15: Variation of the displacement at depths B and 2B with time under a = 0.5 ton, f = 0.5 Hz and R.D. = 80%, under a square surface and embedded footing.

Table 3: Maximum vibration displacement at time17.22 seconds at various load amplitudes, and frequencies

State of soil	Depth	Load amplitude (ton)	Displacement at various frequencies (mm)		
			0.5 Hz	1 Hz	2 Hz
Maximum vibration displacement of surface square footing					
Medium	B	0.5	-29	6.7	6.34
	2B		4.34	4.95	8.15
Dense	B		2.06	4.77	4.02
	2B		-0.98	3.13	4.15
Medium	B	1	5.45	28.23	-----
	2B		0.45	9	-----
Dense	B		5.22	7.28	9.38
	2B		-6.2	4.47	4.99
Maximum vibration displacement of embedded square footing					
Medium	B	0.5	-7.81	9.92	-5.51
	2B		4.04	4.3	1.19
Dense	B		3.2	3.27	-4.32
	2B		1.6	2.31	3.75
Medium	B	1	2.09	9.83	-----
	2B		4.55	6.57	-----
Dense	B		-6.42	-8.13	7.41
	2B		3.66	-5.15	3.95
Maximum vibration displacement of surface circular footing					
Medium	B	0.5	19.19	-15.24	-9

	2B		-10.9	-10.56	19.8
Medium	B	1	-25.88	19.74	------
	2B		-7.07	-14	------
Maximum vibration displacement of embedded circular footing					
Medium	B	0.5	-6.83	-4.36	-12.65
	2B		-1.7	2.62	3.95
Medium	B	1	7.14	7.8	------
	2B		5.23	4.45	------

4. Conclusions

This paper has presented the results of a series of a dynamic load tests to investigate the liquefaction potential of saturated sandy soil under various conditions to study the effect of several parameters that affect liquefaction potential such as load amplitude, relative density, shape of footing, and embedment depth, the following conclusions can be warranted:

1) The surface settlement decreases by increasing the relative density of sand, as well as, the embedment of footing in dense sand reduces the settlement more than medium sand, because the dense soil is the stiffest.
2) The amplitude of displacement decreased at both depths (B and 2B), when soil relative density increased.
3) The settlement of the all tests increased rapidly to reach, at time 17.22 seconds, about (33 – 299) % of the width or diameter of footing used; therefore, the failure has been occurring because of occurrence of final liquefaction in the saturated sand beneath the square and circular footing.

References

[1] Abd Al-Kareem, K. W. (2013), "The Dynamic Behavior of Machine Foundation on Saturated Sand", M.Sc. Thesis, Building and Construction Engineering Department, University of Technology, Iraq.
[2] American Society of Testing and Materials (ASTM) (2006). "Standard Test Method for Specific Gravity of Soil Solids by Water Pycnometer" ASTM D854, West Conshohocken, Pennsylvania, USA.
[3] American Society of Testing and Materials (ASTM) (2006). "Standard Test Method for Particle Size-Analysis of Soils" ASTM D422-02 (2002), West Conshohocken, Pennsylvania, USA.
[4] American Society of Testing and Materials (ASTM) (2006). "Standard Test Method for Maximum Index Density and Unit Weight of Soils Using a Vibratory Table" ASTM D4253-00 (2006), West Conshohocken, Pennsylvania, USA.
[5] American Society of Testing and Materials (ASTM) (2006). "Standard Test Method for Minimum Index Density and Unit Weight of Soils and Calculation of Relative Density" ASTM D4254-00 (2006), West Conshohocken, Pennsylvania, USA.
[6] American Society of Testing and Materials (ASTM) (2006). "Standard Test Method for Direct Shear Test of Soils Under Consolidated Drained Conditions" ASTM D3080, West Conshohocken, Pennsylvania, USA.
[7] American Society of Testing and Materials (ASTM) (2006). "Standard Test Method for Classification of Soils for Engineering Purposes (Unified Soil Classification System)" ASTM D2487-06, West Conshohocken, Pennsylvania, USA.
[8] Aswad, M.F. (2016), "Behavior of Improved Railway Ballast Over Laying Clay Using Geogrid", Ph.D. Thesis, Building and Construction Department, University of Technology, Iraq.
[9] Fattah, M. Y., Al-Neami, M. A., Jajjawi, N. H., (2014), "Prediction of Liquefaction Potential and Pore Water Pressure beneath Machine Foundations", Central European Journal of Engineering, Vol. 4, (3), pp. 226-249. DOI: 10.2478/s13531-013-0165-y.
[10] Fattah, M. Y., Al-Mosawi, M. J., Al-Ameri, A. F. I., (2016), "Dynamic Response of Saturated Soil – Foundation System Acted upon by Vibration", Journal of Earthquake Engineering, 00:1–31, 2016, Taylor & Francis Group, LLC, DOI: 10.1080/13632469.2016.1210060.
[11] Omarov, M. (2010), "Liquefaction Potential and Post-liquefaction Settlement of Saturated Clean Sands: and Effect of Geofiber Reinforcement", Ph.D. Thesis, University of Alaska Fairbanks, USA.
[12] Casagrande, A. (1936), "Characteristics of Cohesionless Soils Affecting the Stability of Slopes and Earth Fills", Journal of the Boston Society of Civil Engineers, reprinted in Contributions to Soil Mechanics, 1925 to 1940, Boston Society of Civil Engineers, Oct., 1940.
[13] Das, B. M. and Ramana, G. (2011), "Principles of Soil Dynamics", Cl Engineering, USA.
[14] GDP-9, G. D. P. (2007), "Liquefaction Potential of Cohesionless Soils State of New York", New York State Department of Transportation.
[15] Sladen, J., D'hollander, R. and Krahn, J. (1985), "The Liquefaction of Sands, a Collapse Surface Approach", Canadian Geotechnical Journal, 22, No. (4), pp. 564-578.
[16] Taiebat, M., Shahir. H., Shahir A. (2007), "Study of Pore Pressure Variation during Liquefaction Using Two Constitutive Models for Sand", Soil Dynamics and Earthquake Engineering, Vol. (27), pp. 60-72.